Title

Monovalent and Multivalent Ligation of the B Cell Receptor Exhibit Differential Dependence upon Syk and Src Family Kinases

Journal

Science Signaling, 6(256)

ISSN

1945-0877

Authors

Mukherjee, Sayak
Zhu, Jing
Zikherman, Julie
et al.

Publication Date

2013

DOI

10.1126/scisignal.2003220

Peer reviewed

Published in final edited form as:
Sci Signal. ; 6(256): ra1. doi:10.1126/scisignal.2003220.

Monovalent and Multivalent Ligation of the B Cell Receptor Exhibit Differential Dependence upon Syk and Src Family Kinases

Sayak Mukherjee[1], **Jing Zhu**[2], **Julie Zikherman**[2], **Ramya Parameswaran**[2], **Theresa A. Kadlecek**[2], **Qi Wang**[3], **Byron Au-Yeung**[2], **Hidde Ploegh**[4], **John Kuriyan**[3], **Jayajit Das**[1,5,6,*], and **Arthur Weiss**[2,*]

[1]Battelle Center for Mathematical Medicine, The Research Institute at Nationwide Children's Hospital, Department of Pediatrics, The Ohio State University, Columbus, OH 43205, USA

[2]The Rosalind Russell Research Center for Arthritis, Department of Medicine, Howard Hughes Medical Institute, University of California, San Francisco, CA 94143, USA

[3]Department of Molecular and Cell Biology, Department of Chemistry, Howard Hughes Medical Institute, University of California, Berkeley, CA 94720, USA

[4]Department of Biology, Whitehead Institute for Biomedical Research, Massachusetts Institute of Technology, Cambridge, MA 02142, USA

[5]Department of Physics, The Ohio State University, Columbus, OH 43205, USA

To whom correspondence should be addressed. aweiss@medicine.ucsf.edu (A.W.); das.70@osu.edu (J.D.).

Competing interests: The authors declare that they have no competing interests.

Supplementary Materials

[6]Department of Biophysics Graduate Program, The Ohio State University, Columbus, OH 43205, USA

Abstract

The Src and Syk families of kinases are two distinct sets of kinases that play critical roles in initiating membrane-proximal B cell receptor (BCR) signaling. However, unlike in other lymphocytes, such as T cells, the “division of labor” between Src family kinases (SFKs) and Syk in B cells is not well separated, because both Syk and SFKs can phosphorylate immunoreceptor tyrosine-based activation motifs (ITAMs) present in proteins comprising the B cell receptor (BCR). To understand why B cells require both SFKs and Syk for activation, we investigated the roles of both families of kinases in BCR signaling with computational modeling and in vitro experiments. Our computational model suggested that positive feedback enabled Syk to substantially compensate for the absence of SFKs when spatial clustering of BCRs was induced by multimeric ligands. We confirmed this prediction experimentally. In contrast, when B cells were stimulated by monomeric ligands that failed to produce BCR clustering, both Syk and SFKs were required for complete and rapid BCR activation. Our data suggest that SFKs could play a pivotal role in increasing BCR sensitivity to monomeric antigens of pathogens and in mediating a rapid response to soluble multimeric antigens of pathogens that can induce spatial BCR clustering.

INTRODUCTION

Unlike most receptor tyrosine kinases, the antigen receptors on lymphocytes require the action of two distinct sets of unlinked cytoplasmic kinases for full initiation of signaling in response to receptor ligation. B cell receptor (BCR) signaling involves the sequential action of the Src family kinases (SFKs) and the kinase Syk (1). After receptor stimulation, membrane-associated SFKs phosphorylate immunoreceptor tyrosine-based activation motifs (ITAMs) of the BCR Igα and Igβ chains. Phosphorylation of both tyrosines in an ITAM leads to the stable recruitment of the cytoplasmic kinase Syk through its tandem Src homology 2 (SH2) domains, which relieves autoinhibitory constraints in Syk and thereby enables SFKs to activate Syk by phosphorylation. Together, these kinases activate downstream signaling events by phosphorylating substrate proteins involved in signaling pathways that result in signal amplification and diversification, with consequent B cell responses. SFKs are themselves tightly regulated by an inhibitory tyrosine near their C-termini and an activation loop tyrosine (2). The inhibitory tyrosine is reciprocally regulated by the kinase Csk and the receptor-like protein tyrosine phosphatases (PTPs) CD45 and CD148. Phosphorylation of this site favors adoption of a closed, inhibited conformation, whereas phosphorylation of the activation loop tyrosine of the SFKs is required for full enzymatic activity.

Syk family kinases are largely regulated through their localization to doubly phosphorylated ITAMs, to which their tandem SH2 domains bind. In addition, their catalytic activity may be activated by catalytic loop phosphorylation by trans-autophosphorylation or by phosphorylation by SFKs. The mechanism of inhibtion of Syk family kinases is not well understood, but binding to the ITAM is likely to relieve an autoinhibitory constraint (3), as it does for the kinase ζ-associated protein of 70 kilodaltons (ZAP-70) (4–6), and further phosphorylation of Syk at sites between the SH2 domains and the kinase domain likely contribute to its activation. Phosphorylation of these sites is likely mediated by SFKs or by Syk through trans-autophosphorylation (7, 8).

By analogy to B cells, T cells also require SFKs and a Syk family kinase to initiate TCR signaling. The T cell–specific Syk family kinase ZAP-70 requires CD45-regulated SFK enzymatic activity to initiate downstream signaling upon receptor ligation (2, 9). Indeed,

mice deficient in either CD45 or the T-cell SFKs Lck and Fyn exhibit a block in TCR signaling and, consequently, thymic development (10–14). Thus, the antigen receptors of B cells and T cells use two families of kinases to initiate receptor-proximal signaling; however, it is not clear why such a "division of labor" has evolved.

The requirement for the two families of kinases in T cells is more readily apparent. In the case of TCR signaling, the SFK Lck is tightly associated with the CD4 and CD8 coreceptors, and this association is required to ensure that recognition is limited to antigenic peptides bound to protein products of syngeneic alleles of the major histocompatibility complex (MHC) (15). Unlike T cells, B cells do not require a particular molecular context to respond to antigen. B cells are capable of recognizing antigens that are either "free" or cell-bound. Thus, B cells are not constrained by the necessity to enlist a coreceptor or to recognize a peptidic antigen that is MHC-bound. Previous studies suggest that B cells, unlike T cells, can signal independently of SFKs, but that they have an absolute requirement for Syk. Kurosaki and colleagues showed in the chicken DT40 B cell line that Syk is required for an induced increase in calcium (Ca^{2+}) mobilization in response to BCR ligation (16). By contrast, the SFK Lyn is dispensable for this event, although Ca^{2+} entry is markedly delayed in its absence.

Consistent with studies in cell lines, fetal liver chimeras generated from Syk-deficient mice revealed that *Syk* $^{-/-}$ B lineage cells in the bone marrow arrest very early in development, at the $CD43^{hi}$ pro-B cell stage (17, 18). This marks the pre-BCR checkpoint and reveals a dependence on Syk for pre-BCR signaling. Because few naïve B cells that express a BCR containing Igμ heavy chains are present in the bone marrow or periphery of *Syk* $^{-/-}$ mice, it is challenging to study mature BCR signaling directly in the remaining Syk-deficient cells. However, introduction of a BCR transgene (Tg) specific for the model antigen hen egg lysozyme (IgHEL Tg) revealed that an increase in Ca^{2+} signaling cannot be induced in response to BCR stimulation in the absence of Syk (19).

SFK-deficient mice, in which all three B cell–specific SFKs, Blk, Lyn, and Fyn, have been deleted, appear to phenocopy Syk deficiency (20). These animals exhibit profound B cell loss at the $CD43^{-}$ pre-B cell stage of bone marrow development. However, quite unexpectedly, stimulation of such triply-deficient pro-B cells with antibody against Igβ (anti-Igβ) revealed no defect in the phosphorylation of Igα, Igβ, Syk, or various downstream targets, such as phospholipase Cγ2, Vav, and Btk. Activation of the transcription factor nuclear factor κB (NF-κB) is impaired in SFK-deficient, but not Syk- deficient, cells. Similarly, mice deficient in the phosphatases CD45 and CD148, whose B cell SFKs are constitutively hyper-phosphorylated at their inhibitory tyrosine phosphorylation sites and thereby inactivated, exhibit an early block in B cell development (21). Nevertheless, despite this inactivation of SFKs, some phosphatase-deficient B cells do develop and exhibit a robust but delayed BCR-induced increase in Ca^{2+} mobilization and protein tyrosine phosphorylation of downstream substrates. Together, these data suggest that Syk is absolutely required for BCR signaling, but that SFKs appear to be dispensable for most downstream signaling pathways, although a delay in signaling events is observed (16, 22).

How does BCR signaling remain largely intact in the absence of SFKs in cell lines and mice? Unlike ZAP-70, Syk is capable of directly phosphorylating ITAMs in the apparent absence of SFKs (23, 24). Moreover, Syk appears to function as a positive allosteric enzyme with increased activity upon binding to phosphorylated tyrosines in ITAMs, thus initiating a positive feedback loop that drives further ITAM phosphorylation (24). An additional feedback loop is triggered by trans-autophosphorylation of the activation loop tyrosine of Syk (25). These observations suggest a possible mechanism for SFK-independent BCR signaling through Syk (24). However, if Syk can signal in response to BCR ligation in the

absence of SFKs, albeit in a delayed manner, why do B cells have SFKs? Clearly, SFK function can accelerate signaling, but what physiological purpose does this serve, and in what contexts does this matter?

B cells, in contrast to MHC-restricted T cells, have the flexibility to recognize both soluble monomeric and multimeric ligands. The latter induce clustering of multiple BCRs, while the former presumably do not. We have developed a mathematical model of proximal BCR signaling to define the relative contributions of Syk and the SFKs to BCR ligation by monomeric versus multimeric ligands. Our model predicts that although monomeric BCR ligation is heavily dependent on SFK activity, BCR clustering by multimeric ligands frees the cell from a strict dependence on SFKs. Under these circumstances, Syk activity alone is sufficient to trigger signaling, albeit in a delayed manner. We tested this model by evaluating the effects of selective inhibition of SFK and Syk on primary murine B cells in the context of BCR clustering versus monomeric BCR ligation. We confirmed the predictions of our model and showed that minimal assumptions regarding the ability of Syk to produce robust ITAM phosphorylation in the presence of BCR clustering are required, even in the absence of SFKs. Our studies unmasked physiologically relevant circumstances under which SFK function was crucial during BCR signaling. We propose that dual kinase–dependence of BCR signaling may have evolved for two reasons: to permit rapid responses upon BCR clustering and to facilitate the increased sensitivity that is needed for the recognition of soluble monomeric ligands by the BCR.

RESULTS

Compensation for the absence of SFKs by the kinase Syk when BCRs are clustered

We constructed a computational model to investigate the role of BCR clustering on ITAM phosphorylation mediated by SFKs and Syk family kinases. The spatially inhomogeneous *in silico* model explicitly accounts for the diffusion of molecules in the plasma membrane and the cytosol, as well as the stochastic nature of the biochemical reactions that result because of small variations in the copy numbers of signaling molecules. We performed a continuous time Monte Carlo (Gillespie simulation) to solve the Master equation associated with the reaction diffusion events in the signaling network. We modeled the biochemical signaling reactions and spatial movements of molecules occurring at the interface of the B cell plasma membrane and the cytosol. In our simulations, we considered a three-dimensional (3D) region in the B cell that contained a 23-μm^2 area in the plasma membrane and a membrane-proximal cytosolic region with a height of 0.044 μm beneath the plasma membrane (Supplementary Materials, section 1 and fig. S1). This region was divided into smaller cubic chambers, or subvolume units (fig. S1), in which the time scales associated with diffusion of the molecules are faster than those of the reactions, and consequently, molecules could be considered well mixed in each subvolume unit. The diffusion of the molecules was simulated by the hopping of molecules from a subvolume unit to one of its nearest neighbor subvolumes, which is represented by a first-order chemical reaction occurring at a rate of D/l^2, where l is the length of a side of the cubic subvolume, and D is the diffusion coefficient of the diffusing molecule.

In our models, we specifically considered interactions between the BCR and soluble monomeric and dimeric hen egg lysozyme (HEL) antigens. The precise mechanisms underlying BCR triggering in response to interactions with soluble antigens are not well-understood (26). Imaging experiments have been used to study early signaling events in BCR triggering for membrane-bound antigens. Various competing mechanisms have been proposed to explain results from those experiments, including: Cμ4 domain– mediated BCR clustering by surface-bound antigens (27); conversion of auto-inhibited BCR clusters into activated monomers or smaller clusters after antigen binding (28); and actin-induced

organization of BCR clusters leading to ITAM phosphorylation (26). However, here, we did not aim to investigate different molecular mechanisms of BCR triggering. Rather, we studied the functional consequences of having smaller BCR clusters containing one or two antigen-bound BCRs or having larger clusters with many BCRs. In our model, BCRs interact with stimulatory antigen molecules (Fig. 1). The monomeric antigens produced signaling-competent monomers of BCR-antigen complexes. We also studied signaling in which ITAM phosphorylation was initiated upon formation of a dimer (BCR-antigen-BCR-antigen) of BCR-antigen complexes in which BCRs were stimulated by monomeric antigens to study the role of BCR oligomerization in BCR triggering as proposed by a mechanism such as Cμ4 domain–mediated BCR clustering; but, these did not lead to any qualitative changes to the results (Supplementary Materials, section 2, fig. S2, showing qualitatively similar results as compared to Fig. 2A and 2B, and movie S1).

In contrast, dimeric antigens were assumed to generate BCR microclusters. We modeled a microcluster by confining signaling-competent, antigen-bound BCRs in a 2.0-μm^2 region (29, 30). Our models, including dynamically induced clustering of the antigen-bound BCRs into the microclusters, did not produce any qualitative changes in the results other than slowing the BCR activation kinetics (see Supplementary Materials, section 2, fig. S3, and movies S2 and S3 for details). Therefore, for simplicity, we present results using a preformed BCR microcluster. Dimeric antigens induce clustering of BCRs by cross-linking BCRs in a process by which each epitope binds to one BCR. This could produce BCRs clusters of different sizes (for example, dimers, trimers, etc.). Because the main purpose of our modeling is to investigate how membrane-proximal signaling through SFKs and Syk is influenced by the spatial clustering of ITAMs initiated by multivalent ligands, we did not include explicit multimerization of BCRs. Thus, the coarse-grained model probes the effect of a BCR microcluster generated by dimeric antigens without considering more microscopic details of BCR clustering, that is, the presence of BCR dimers, trimers, or higher-order multimers. This approximation also keeps the models computationally feasible without sacrificing the general features of the models. We briefly describe the signaling reactions and diffusion below.

Each BCR is associated with a pair of ITAMs. Upon binding of BCRs to stimulatory antigens, the tyrosine residues in the ITAMs are phosphorylated by activated forms of SFKs, such as Lyn. When both of the tyrosine residues in an ITAM are phosphorylated, Syk binds to the ITAM through its tandem SH2 domains with a relatively strong affinity (dissociation constant, K_d ~ 640 nM) (31). We have assumed that when the tyrosine residues in ITAMs are bound to the SH2 domains of Syk, they are protected from dephosphorylation by phosphatases. This assumption is supported by later experiments and from published studies with ZAP-70 (32). Partially phosphorylated ITAMs, in which one of the two tyrosine residues is phosphorylated, recruit Syk with a much weaker affinity (K_d ~ 32 μM) (31). Syk undergoes autophosphorylation at Tyr^{348} (Y348) and becomes catalytically active (33).

We also investigated the role of SFKs in phosphorylating the activation loop of Syk (fig. S4), which did not change the qualitative features of the results. Therefore, for simplicity, we do not include this signaling event in the model. In addition, we approximated the number of possible ITAM activation states that a BCR can assume to keep the computation within a feasible range (see Supplementary Materials, section 3, and, fig. S5). Catalytically active Syk, unlike ZAP-70, can also trans-phosphorylate basally active Syk bound to a neighboring ITAM (33). This constitutes a positive feedback loop. Moreover, Syk, when bound to an ITAM, can also phosphorylate ITAMs that come in contact with its kinase domain, including ITAMs associated with neighboring BCRs, perhaps brought into proximity by multivalent ligands (24). This produces a second positive feedback loop, because fully phosphorylated ITAMs will robustly recruit additional Syk molecules, thereby

inducing more ITAM phosphorylation. The SH2-containing phosphatase-1 (SHP-1) binds to phosphorylated-ITAMs (pITAMs) or coreceptors (such as CD22) through its tandem SH2 domains. Receptor-bound SHP-1 dephosphorylates pITAMs (34).

We have a negligible amount of serial triggering of BCRs (a single antigen activating ITAMs associated with multiple BCRs) in our model because of the long half life (~3.3 min) of antigen-BCR complexes (more details in Supplementary Materials, section 4, and fig. S6). This is consistent with experiments that suggest the absence of serial triggering in BCR signaling (35). We used high-affinity ligands (HEL, K_D ~0.02 nM) (36, 37) in experiments that are consistent with the simulations performed with high-affinity ligands that produce very little serial triggering. Serial triggering could potentially play a role in BCR stimulation by lower affinity ligands; however, kinetic proof-reading appears to play a dominant role over serial triggering for B cell activation (38–40). We have investigated the sensitivity of our main results for lower-affinity ligands (Fig. 2 and fig. S7). There is very strong evidence supporting the notion that tonic BCR signaling occurs in the absence of added ligand (41–43). This might occur through monomeric BCRs or pre-existing microclusters, possibly because of interactions that occur due to some low concentration of antigen. We used first-order reactions producing low amounts of ITAM phosphorylation and dephosphorylation to represent such tonic signaling. We also performed simulations with a small number of activated ITAMs to represent such basal activation. The qualitative features of our results do not change in the presence of such an initial concentration of ITAMs (see Supplementary Materials, section 5, and, fig. S8). In addition to these considerations, SFKs and unbound BCRs diffuse with a diffusion constant D of ~0.01 $(\mu m)^2/s$ in the plasma membrane (44), and unbound Syk and SHP-1 molecules diffuse in the cytosol with a faster diffusion rate (D ~ 10.0 $(\mu m)^2/s$) (45, 46). More details are provided in the Materials and Methods and the Supplementary Materials (fig. S1, and tables S1 and S2).

We investigated the effects of spatial BCR microclusters in the *in silico* model by considering two scenarios. In the first scenario, BCRs form microclusters after antigen binding. In this case, we studied the kinetics when there is a preformed microcluster of BCRs with its multivalent ligands. In the second scenario, BCRs do not form microclusters. We studied the kinetics of ITAM phosphorylation when BCRs are stimulated by strong affinity antigens (with a half-life ~3.3 min). The concentrations of fully phosphorylated ITAMs serve as markers for activation, because the downstream activation of various targets, such as the adaptor protein BLNK, Bruton's tyrosine kinase (Btk), the Rho-family guaninine nucleotide exchanger factor (GEF) Vav, and Ca^{2+} influx are dependent on the production of fully phosphorylated ITAMs. When BCRs formed a microcluster, the activation of the ITAMs did not show a large decrease in magnitude in the absence of SFKs (Fig. 2A). In contrast, if a microcluster was unable to form, ITAM phosphorylation decreased substantially in the absence of SFKs (Fig. 2B). These results suggest that Syk can partially compensate for the absence of SFK activity in the presence of receptor clustering. However, the SFKs were not able to restore ITAM phosphorylation in the Syk-deficient system regardless of the nature of spatial clustering of the BCRs (Fig. 2C and D).

These results can be mechanistically understood in the following way. When Syk molecules are recruited by BCRs in a microcluster, they can phosphorylate the neighboring ITAMs, which in turn can recruit more Syk molecules to the microcluster to stimulate further ITAM phosphorylation. This positive feedback loop in ITAM activation helps the Syk molecules counteract the absence of any SFK activity. However, when BCRs are prevented from forming a microcluster, an ITAM-bound Syk molecule has access to a much smaller number of nearby ITAMs. Therefore, the effect of the positive feedback loop is much reduced in the absence of spatial clustering (Fig. 2B). In contrast, SFKs are unable to mediate such a positive feedback and consequently cannot restore activation in Syk-deficient systems,

which leads to a large decrease in the extent of ITAM phosphorylation irrespective of whether the receptor is clustered (Fig. 2C and 2D). We note that SFKs can bind to singly phosphorylated ITAMs with a single SH2 domain with a very weak affinity that is about 100- to 1000-times weaker than the binding affinity of the tandem SH2 domains of Syk for fully phosphorylated ITAMs. Therefore, the contribution of SFKs to the phosphorylation of neighboring ITAMs is small, and our calculations showed that including this reaction did not change the results qualitatively (see Supplementary Materials, section 6, and, fig. S9).

We next investigated how Syk-mediated positive feedback was influenced by different concentrations of antigens. In the presence of microclusters, the Syk-mediated feedback compensated for the absence of SFKs in activating ITAMs for a wide range of antigen concentrations (Fig. 2E). In contrast, in the absence of any receptor clustering, Syk-mediated feedback was unable to restore ITAM activation in the absence of any SFK activity over a large range of antigen concentrations. However, at increased antigen concentrations, the Syk-mediated feedback partially restored ITAM activation in the SFK-deficient system (Fig. 2F). This occurred because at increased antigen concentrations, even in the absence of any receptor clustering, ITAM-bound Syk molecules are likely to engage with and phosphorylate ITAMs associated with nearby BCR-antigen complexes.

We also found that the threshold for ITAM activation in the SFK-deficient system occurred at a slightly increased antigen concentration as compared to that in the wild-type system (Fig. 2E and 2F). This change in the threshold of activation in the SFK-deficient system was more substantial in the absence of any spatial clustering (Fig. 2E). This can be understood in the following way. In the absence of any SFK activity, the first few ITAMs that help to initiate the Syk-induced positive feedback are activated by basally activated Syk molecules, which are less efficient in phosphorylating ITAMs compared to the SFKs; therefore, the amount of antigen required to induce the positive feedback loop in the wild-type system is smaller than that in SFK-deficient systems. Because in the absence of receptor clustering the positive feedback can be effectively employed only at increased antigen concentrations, the threshold for ITAM activation occurs at a much higher antigen concentration in the absence of any SFK activity in this case. The Syk-mediated positive feedback can also give rise to bistability in ITAM phosphorylation for a range of antigen concentrations and reaction rates. The bistability occurs because of nonlinearity in feedback-induced ITAM phosphorylation and enzymatic dephosphorylation of ITAMs (see Supplementary Materials, section 7, and, figs. S10–12 for more details). We also investigated the role of BCR spatial clustering for weaker affinity antigens ($k_{off} \sim 0.05s^{-1}$ to $0.5s^{-1}$). For moderate affinity antigens ($k_{off} \sim 0.05\ s^{-1}$), ITAM activation in the absence of SFKs was partially restored by Syk-mediated feedback in the presence of BCR clustering (Fig. 2G and 2H). However, for lower affinity ligands ($k_{off} \sim 0.5\ s^{-1}$), in the absence of SFKs, Syk was not able to restore ITAM activation, because the lifetime of the BCR-antigen complex becomes too short to generate ITAM activation through Syk (fig. S7C and S7D).

We directly tested the role of positive feedback in ITAM activation mediated by Syk through its ability to phosphorylate neighboring ITAMs. We modified our computational model such that Syk molecules were not allowed to phosphorylate any neighboring ITAMs. We then studied the kinetics of ITAM phosphorylation when either SFK or Syk molecules are removed from the system. In the absence of SFKs, the concentrations of pITAMs decreased substantially both in the presence and absence of any receptor microcluster (Fig. 3A and 3B). The concentration of pITAMs, even in the wild-type system, was substantially reduced in this modified model compared to that in the original model in which Syk-induced positive feedback was functional. In the modified model, when Syk was not present, ITAM phosphorylation was reduced by a small amount regardless of the degree of spatial clustering of BCRs (Fig. 3C and 3D). This occurred because ITAM phosphorylation by the

SFKs was not affected by spatial clustering. Increasing the antigen concentration increased the amount of ITAM phosphorylation in the modified model in a graded manner; however, overall, the magnitude of ITAM phosphorylation was substantially reduced compared to that in the original model (Fig. 3E and 3F). Even at increased concentrations of antigens, the modified model in the absence of any receptor clustering showed a large decrease in activation when SFKs were absent. This is in contrast with the original model in which, at increased antigen concentrations, Syk-mediated positive feedback compensated for the absence of SFKs in the presence of receptor clustering (Fig. 3E and 3F). To summarize, our *in silico* simulations predict that in the presence of receptor clustering, Syk substantially compensates for the absence of SFKs and induces ITAM phosphorylation to almost the same extent as occurs when Syk and SFKs are present.

Enzymatic activities of purified recombinant SFK and Syk kinases for ITAM- and LAT-based substrates

Much of our understanding of the specificities of SFKs and Syk family kinases for ITAMs is based on genetic mutants or cell-based over-expression systems (24, 47–53). Because the interpretation of results obtained in such cellular systems may be compromised by the presence of low amounts of endogenous SFKs, Syk family kinases, or other kinases that might function in ITAM-based or downstream signaling, we studied the substrate specificity of purified recombinant Syk, ZAP-70, and Src proteins. We used a T cell receptor ζ (TCRζ)-derived peptide as the prototypical ITAM substrate, and a peptide derived from the adaptor molecule LAT as the Syk family kinase substrate, because phosphorylation of these peptides is readily detectable in our experimental system. Activated recombinant purified Syk and ZAP-70 proteins phosphorylated LAT with similar Km and Kcat values, whereas purified Src had much less specificity for LAT (Fig. 4). In contrast, Src had much greater specificity for the *in vitro* phosphorylation of ITAM tyrosines compared to that of ZAP-70. Additionally, Syk had intermediate specificity for ITAM phosphorylation. These results support the notion that Syk can phosphorylate ITAMs, not as well as Src, but far better than can ZAP-70.

Experimental tests in cells of the *in silico* model prediction

To test our computational model in cells, we first examined the relative capacity of ZAP-70 and Syk to phosphorylate ITAMs in the absence or presence of SFK activity when either Syk family kinase was over-expressed in a heterologous cell system. Human embryonic kidney (HEK) 293T cells were transiently transfected with plasmids encoding ZAP-70 or Syk together with a model substrate ITAM, a plasmid encoding the dimeric chimeric CD8ζ chain protein, in the presence or absence of plasmid encoding the SFK Lck. The TCRζ chain contains three ITAMs, and its phosphorylation is readily detected by Western blotting. Consistent with previous studies, we found that Lck alone phosphorylated the ITAMs (Fig. 5A, right panel). In contrast, and consistent with previous studies, ZAP-70 was unable to phosphorylate these ITAM tyrosine residues in the absence of Lck (Fig. 5A, left panel). However, TCRζ ITAM phosphorylation was readily detected in the presence of Syk without concomitant over-expression of Lck (Fig. 5A, left panel), suggesting that Syk was capable of independently phosphorylating these sites. Syk-mediated phosphorylation of ITAMs was dependent on the SH2 domains of Syk, consistent with one of the positive feedback loops discussed in our proposed computational model. To control for the contribution of endogenous SFK activity in the HEK 293T cells, we took advantage of PP2, which is a well-established SFK inhibitor with high specificity within the IC_{50} range of 4 to 5 nM for SFKs as compared to >100 μM for ZAP-70 (54). In the presence of PP2, expression of neither Lck nor ZAP-70 led to TCRζ ITAM phosphorylation, but Syk continued to do so (Fig. 5A). Consistent with previous work, these data demonstrate a critical difference between ZAP-70 and Syk substrate-selectivity with implications for antigen receptor signaling in T and B

cells. To confirm that the ITAM phosphorylation mediated by Syk was indeed a result of Syk catalytic activity, we used the Syk inhibitor BAY 61–3606, which is Syk-selective relative to SFKs (55). Indeed, BAY 61–3606 inhibited Syk-mediated, but not Lck-mediated, phosphorylation of ITAMs (Fig. 5B). These results suggest that Syk mediates the phosphorylation of ITAMs independently of SFKs, and that its SH2 domains are required for this activity.

Role of SFKs and Syk in BCR signaling in primary mouse B cells

These heterologous expression studies suggested that Syk phosphorylated ITAMs, and they implied that Syk should be sufficient to mediate BCR signaling in primary B cells in the absence of SFKs. However, this is difficult to assess directly because B cell development in Syk-deficient or SFK-deficient mice is severely impaired, with nearly complete blocks at the pre-B bone marrow stage, which precedes expression of the BCR (17, 18, 20). To circumvent these impairments in B cell development, we first used inhibitors to assess the requirements for SFK and Syk catalytic activity during BCR signaling in primary mature mouse B cells. To directly test the predictions of our model, we took advantage of the SFK inhibitor PP2 and the Syk inhibitor BAY 61–3606 in an *ex vivo* primary B cell system. We confirmed the relative specificities of these inhibitors by comparing their effects on BCR- and TCR-induced increases in cytoplasmic Ca^{2+}. B cells have Syk but not ZAP-70, whereas T cells have ZAP-70, but not Syk. Therefore, we would not expect the Syk-specific inhibitor BAY 61–3606 to influence TCR signaling. Indeed, BAY 61–3606 had no effect on TCR-induced Ca^{2+} flux, whereas inhibition of SFK activity with PP2 completely abolished TCR-induced Ca^{2+} mobilization (Fig. 6A). In contrast, BCR-induced increases in Ca^{2+} flux were sensitive to Syk inhibition, whereas the same concentration of PP2 that blocked TCR-induced Ca^{2+} flux delayed, but did not abolish, BCR-induced Ca^{2+} signaling (Fig. 6B). These data are consistent with our model and suggest that Syk has the capacity to phosphorylate ITAMs in the absence of SFK activity, and that it can thereby initiate downstream signal transduction.

Our model predicts that the dependence of BCR signaling upon SFK activity is mostly influenced by BCR clustering (Figs. 2 and 3), and this could explain the time-dependency of the BCR response in the presence of SFK inhibition; that is, clustering of BCRs in the membrane by multivalent ligands would be expected to be associated with a time delay in response. To test this prediction, we took advantage of the MD4 BCR transgenic system in which primary mouse B cells express a monoclonal BCR that specifically recognizes the model antigen hen egg lysozyme (HEL) (56). Previously, Kim *et al.* multimerized soluble HEL (sHEL) by gluteraldehyde-mediated cross-linking (57). We used monomers of HEL and glutaraldehyde-crosslinked dimers of sHEL to compare BCR signaling under monomeric versus clustering conditions, and we examined the dependency of the BCR responses upon the activities of SFK and Syk to these forms of HEL. As predicted by our model, we found that stimulation of MD4 B cells by monomeric sHEL was sensitive to the inhibition of either Syk or SFK (Fig. 6C). However, stimulation with dimeric sHEL resembled that with anti-IgM (bivalent antibody-mediated), such that SFK inhibition delayed, but did not completely eliminate, Ca^{2+} mobilization (Fig. 6D). In contrast, inhibition of Syk completely inhibited the response to dimeric sHEL (Fig. 6D). These data suggest that although the kinase activities of SFKs play a role in both monomeric and multimeric BCR signaling, the former condition is much more sensitive to SFK inhibition.

We extended these observations to B cells with genetically impaired SFK function. Previously, we showed that disruption of two phosphatases, CD45 and CD148, resulted in marked impairment of SFK activity in B cells because of the enhanced phosphorylation of the inhibitory tyrosine and the consequent allosteric inhibition of the SFKs (21). Deficiency in both CD45 and CD148 results in an early, but incomplete, block in B cell development,

which enabled us to study these double knockout (DKO) B cells. Such DKO B cells exhibit an impairment in Ca^{2+} mobilization after BCR stimulation (21). This Ca^{2+} response is not completely abolished, but is delayed in a manner reminiscent of that in PP2-treated B cells (15). We were interested in whether the previously observed residual increased in Ca^{2+} mobilization in CD45 and CD148 DKO B cells was attributable to SFK-independent Syk activity. To examine this, we generated mixed bone marrow chimeras containing both DKO (CD45.1−) and wild-type (CD45.1+) B cells. The congenic CD45 markers enabled us to monitor the BCR-induced Ca^{2+} response in both the wild-type and DKO cells concurrently. We induced BCR clustering with anti-IgM and observed delayed Ca^{2+} flux in DKO B cells, which contrasted with the rapid response that we observed in wild-type B cells (Fig. 7). As expected, SFK inhibition with PP2 did not further dampen Ca^{2+} mobilization in DKO B cells (Fig. 7A). Instead, we found that inhibition of Syk in DKO B cells with BAY61–3606 completely abolished the delayed Ca^{2+} mobilization induced by BCR stimulation (Fig. 7B). Considering results from both the chemical and genetic perturbation of SFK activity, our experimental data support predictions derived from our model that BCR clustering renders B cells relatively independent of SFK kinase activity but highly dependent on Syk activity. Moreover, our data suggest that SFK activity serves to increase the kinetics and sensitivity of BCR responses to less multivalent ligands.

DISCUSSION

ITAM-coupled receptors in cells of the hematopoietic lineage that recognize model antigen or pathogen-derived antigens use two families of cytoplasmic kinases to initiate signaling through tyrosine phosphorylation pathways. The reason for this division of labor is most apparent in the case of TCR function, that is, to couple SFK (Lck) activity to coreceptor- and TCR-mediated recognition of antigenic peptide-bound MHC. Indeed, in the case of T cells, the second kinase ZAP-70 is completely dependent upon SFKs for recruitment to the TCR or activation (48, 50, 51). However, B cells and other hematopoietic cells also use ITAM-coupled receptors, but the purpose for the division of labor between the two families of kinases is not so apparent. Previous studies and our findings here have shown that Syk can phosphorylate ITAMs and initiate signaling independently of SFKs (24, 52). What then is the purpose of involving SFKs upstream of Syk? Our modeling studies and experimental work suggest that SFKs serve to increase the sensitivity of the BCR, and likely those of other ITAM-coupled receptors that use Syk, to stimulation by soluble ligands that are less multivalent. This increase in sensitivity has importance in providing protection from pathogens that do not display highly polymeric antigens or ligands.

Although we and others have shown here and elsewhere that Syk phosphorylates ITAMs (23, 24), based on *in vitro* kinetic parameters provided herein, it does so less efficiently than do SFKs. Syk appears to depend heavily on the presence of its SH2 domains for ITAM phosphorylation. This may be due to the protection of pITAMs from protein tyrosine phosphatases, as well as the localization and concentration of Syk catalytic function at the tyrosines of nearby ITAMs. As presented in our model, and supported by experimental data, the combination of such non-catalytic Syk function can produce potent positive feedback.

Our modeling studies highlight the role of receptor multimerization in triggering positive feedback loops that serve to drive ITAM phosphorylation and Syk activation even in the absence of SFKs. However, this process remains relatively inefficient in the absence of SFKs and renders BCRs relatively insensitive to soluble monomeric ligands. This was most apparent in our studies comparing monomeric and dimeric sHEL. In the absence of SFK function, no response to monomeric sHEL was detected. There are many pathogens that display oligomeric antigens on their surfaces, such as bacteria and viruses. However, some monomeric pathogen-derived products, such as toxins, may be less capable of triggering B

cell responses but responses to these antigens are important in protecting the host. It is likely that such responses will be much more highly dependent on SFK participation in BCR signaling.

Why are SFKs so important? The need for receptor clustering in the absence of SFKs imposes a delay upon the initiation of responses until BCRs can be brought into clusters by multivalent ligands. For weak ligands, dissociation may occur before clustering can occur or signaling is initiated, thereby impairing B cell responses to such ligands. In the presence of SFK function, BCR signaling can be initiated more rapidly and with greater sensitivity to less oligomeric ligands. Thus, SFK function is not absolutely necessary to initiate a BCR response, but primarily serves to increase the sensitivity of the immune system to antigen stimulation, especially to low-affinity interactions and to less oligomeric antigens.

These modeling studies and experimental data have implications for the resistance to pathogens and responses of other hematopoietic cells. Based on our work, we would predict that SFK-deficient or CD45- and CD148-deficient mice have a particularly increased susceptibility to pathogens (or their toxic products) that do not display highly polymeric antigens on their surfaces. We would also predict that other cell types might have alterations in the sensitivities of their ITAM-coupled receptors to activation in the absence of SFK function. For example, SFK-deficient or CD45- and CD148-deficient natural killer cells may be much more resistant to activation as the concentration of activating ligand decreases. Further work will be necessary to explore these predictions.

MATERIALS AND METHODS

Stochastic simulation

We performed a continuous-time Monte Carlo (MC) simulation (Gillespie Method) (58) that solves the Master equation that describes stochastic biochemical reactions associated with the model and diffusive movements of the molecules on the plasma membrane and in the cytosol. We used a simulation box of an area ($\boldsymbol{L} \times \boldsymbol{L}$) of 23 μm^2, which is roughly equal to 20% of the B cell surface (127 μm^2). The height ($\boldsymbol{l}$=0.044μm) of the simulation box represents the interface between the plasma membrane and the cytosol where the signaling molecules can interact. The entire simulation box is divided into small sub-volume units of size ($\hat{l}^3$, $\hat{l}$=0.044 μm) such that the signaling molecules are well mixed in the sub-volume units. The antigens interact with the BCRs above the interface between the plasma membrane and the cytosol within a layer of height (l = 0.044μm). This region is also divided into small sub-volume units of size $\hat{l}^3$. We used the Stochastic Simulation Compiler (SSC) software package (59) to carry out the MC simulations. The codes used for the simulation are available at: http://planetx.nationwidechildrens.org/~jayajit/. Further details regarding the method and the parameters used can be found in the Supplementary Materials, Sections 1 and 2, figs. S1 to S3, table S1 and S2. We also performed a parameter sensitivity analysis of the results shown in Figs. 1 and 2. The details are provided in tables S3 and S4, and in figs. S13 to S22.

Coupled kinase assay

A continuous pyruvate kinase–coupled assay was performed to measure the kinase activities of the proteins as described previously (60), with minor medications. The ATP concentration was kept at 1 mM in all of the assays. The buffer used contains 10 mM $MgCl_2$, 25 mM tris-HCl (pH 7.5), 2 mM sodium orthovandate. The protein concentrations were kept at 1 μM for all three kinases. The reactions were performed in a 96-well plate and were monitored by SpectraMax (Molecular Devices). For substrate titration experiments, the initial reaction velocity (Vo) was measured in triplicate over 10 different substrate

concentrations ranging from 50 μM to 3 mM. The curves were fitted into Michaelis Menten kinetics equation with software Origin: Vo = Kcat[Eo][S]/(Km+[S]),where [Eo] and [S] denote kinase and substrate concentrations, respectively.

Protein expression and purification

DNA encoding human Syk (amino acid residues 1 to 628) was cloned into pFastBac 1 (Invitrogen) with a Gly-Ser-Gly linker, a PreScission protease site, and a six-histidine tag at its C-terminus. Recombinant bacmid DNA containing the Syk insert was prepared in the Bac-to-Bac expression system (Gibco BRL), and was used to transfect TriEx Sf9 cells. Baculovirus obtained from the transfected cells was used to infect TriEx Sf9 cells grown in suspension. Cells were harvested 48 hours after infection by centrifugation at 1800*g* and resuspended in phosphate-buffered saline (PBS, Invitrogen). Cells were lysed with a French press and centrifuged at 100,000g for 1 hour to remove cellular debris. The soluble fraction of the lysate was filtered and applied to a 5-ml HisTrap Ni-NTA column (GE Healthcare). The column was then washed with 100 ml of Ni-NTA buffer A containing 20 mM tris, 500 mM NaCl, and 20 mM imidazole. Protein was eluted with a linear imidazole gradient (20 to 500 mM), and the Syk-containing fractions were pooled, buffer-exchanged into PBS, and incubated overnight with PreScission protease at 4°C. The solution was then applied to a HisTrap Ni-NTA column (GE Healthcare) again to remove protease and the cleaved histine-tag. The flow through was concentrated to a volume of 3 ml and further purified by Superdex 200 column (GE Healthcare) in a buffer containing 20 mM tris, 400 mM NaCl, and 2 mM TCEP. The Syk-containing fractions were then pooled, concentrated with an Amicon Ultra Centrigugal Filter device (10 kD cutoff, Millipore) to a final concentration of 5 mg/ml, flash frozen by liquid nitrogen, and stored at −80°C. ZAP70 was generated and purified as described previously (5).

Preparation of c-Src protein

DNA encoding chicken c-src (amino acid residues 83 to 534) was cloned into the pProEX HTb expression plasmid (Invitrogen) to generate N-terminally 6-histidine-tagged fusion protein. The hexahistidine-tag was cleavable by PreScission protease. For protein expression, BL21 DE3* (Novagen) cells were transformed with the plasmid and were then grown in Terrific Broth (TB) medium supplemented with ampicillin (50 mg/l) at 37°C. When the culture reached a cell density corresponding to an absorbance of 0.8 at 600 nm, the temperature was reduced to 18°C, and protein production was induced with 1 mM IPTG. After 16 hours, cells were harvested by centrifugation, resuspended in Ni-NTA buffer A, and flash-frozen in liquid nitrogen. After cell lysis by French press and removal of cell debris by centrifugation, clear lysates were loaded onto a HisTrap Ni-NTA column (GE Healthcare), washed by 100 ml of Ni-NTA buffer A. Proteins were eluted on a single step of NiNTA buffer A supplemented with 250 mM imidazole. Proteins were buffer exchanged into storage buffer [25 mM tris-HCl (pH 8.0), 400 mM NaCl], and affinity tags were removed by incubation with the PreScission protease at 4°C overnight. Cleaved proteins were collected in the flow-through during NiNTA affinity chromatography, and were subjected to size-exclusion chromatography on a Superdex 200 column (GE Healthcare) equilibrated in storage buffer. Proteins were concentrated on an AmiconUltra Centrigugal Filter device (10-kD cutoff) to a final concentration of ~30 mg/ml. Protein aliquots were frozen in liquid nitrogen and stored at −80°C.

Preparation of active ZAP-70 and Syk

10 μM purified ZAP-70 or Syk protein was incubated with 500 nM six-histidine-tagged c-Src kinase domain at room temperature for 2 hours in reaction buffer containing 100 mM NaCl, 25 mM tris-HCl (pH 7.5), 2 mM sodium vanadate, 10 mM $MgCl_2$, and 1 mM ATP. The reaction was completed within 2 hours. The reaction mix was then loaded onto a 1-ml

HisTrap Ni-NTA column (GE Healthcare) to remove the six-histidine-tagged c-Src kinase domain. The flow through containing activated ZAP-70 or Syk was then used for functional studies.

Mice

$CD148^{tm-/tm-}$ $CD45^{-/-}$ DKO mice have been described previously (22), as have IgHEL (MD4) mice (56). C57BL6 and congenically marked $CD45.1^{+}$ BoyJ mice were obtained from Jackson Labs. All knockout and transgenic strains were fully backcrossed to the C57BL/6 genetic background. Mice were used for all functional and biochemical experiments at 5 to 9 weeks of age. All mice were housed in a specific pathogen-free facility at University of California San Francisco in accordance with the university's Animal Care Committee and National Institutes of Health guidelines.

Antibodies

Antibodies with the following specificities were used for staining mouse cells: CD4, CD21, CD23, panCD45, CD45R, and CD45.1. Monoclonal antibodies (mAbs) conjugated to FITC, PE, PerCP-Cy5.5, PE-Cy5.5, PE-Cy7, Pacific blue, APC, Alexa 647, or Qdot-605 were purchased from commercial sources (eBiosciences, BD Biosciences, Biolegend, or Invitrogen). The following antibodies were used for the stimulation of lymphocytes: hamster mAb against CD3ε (2C11); goat anti-Armenian hamster IgG(H+L) antibody, and goat anti-mouse IgM, (Jackson Immunoresearch). The following antibodies were used for Western blotting analysis: anti-phosphotyrosine mAb 4G10 was purchased from Upstate Biotechnology, and mAbs 2F3.2 (anti−ZAP-70), 4D10 (anti-Syk), 1F6 (anti-Lck), and 6B10 (anti-TCRζ) have been described previously (61, 62).

Stimuli and inhibitors

Monomeric and dimeric forms of HEL (Sigma) were prepared as previously described (57). PP2 (cat#529573) and the Syk inhibitor IV Bay 61–3606 (cat#574714) (Calbiochem) were used at various concentrations to inhibit SFK and Syk kinase activity, respectively.

HEK 293T cell overexpression system

HEK 293 cells (a kidney epithelial cell line) were transiently transfected with various combinations of plasmids (pDNA3-based, Invitrogen) encoding human Lck, ZAP-70, Syk, SH2-mutated Syk, and CD8ζ as previously described (63). Immediately after transfection, cells were incubated in medium in the presence or absence of 20 μm PP2 and 1 μM Bay 61–3606 for 12 hours. Cells were lysed on ice in 1% NP40 alternative lysis buffer (50 μl per well of HEK 293 cells), and cellular debris was removed by centrifugation at 15,000g for 15 min at 4°C). Supernatants were diluted in an equal volume of SDS sample buffer and analyzed by SDS-polyacrylamide gel electrophoresis (SDS-PAGE) and Western blotting with primary and horseradish peroxidase (HRP)-conjugated secondary antibodies. Proteins were then detected by chemiluminescence (Western Lightning; Perkin-Elmer) on a Kodak Image Station.

Ca^{2+} flux assays

Single-cell suspensions of total splenocytes or lymphocytes were loaded with Indo-1 AM (Invitrogen) at a concentration of 10^7 μg per 5×10 cells per ml in "calcium-flux media" (RPMI containing 10 mM Hepes and 5% fetal calf serum (FCS) for 30 min at 37°C in the dark. Cells were subsequently washed and stained with antibodies specific for CD23 and CD4 on the cell surface to identify B cells and T cells, respectively. Cells were resuspended in calcium-flux media at a final concentration of 10^7 cells/ml and then were stimulated at 37°C with various concentrations of BCR- or TCR-specific stimuli in the presence or

absence of inhibitors as noted in the figures. Stimuli and inhibitors were added simultaneously as noted by arrows in figures. The ratio of Ca^{2+}-bound and –unbound Indo-1 was assessed by flow cytometry (BD LSR-Fortessa). Kinetic analysis was performed with Flowjo v8.8.4 software (Treestar).

Generation of BM chimeras

BM chimeras were generated by the transfer of wild-type and DKO BM into lethally irradiated Ly5.1 recipients at a 1:1 ratio, as previously described (22). Recipients were sacrificed 6 to 8 weeks later.

Supplementary Material

Refer to Web version on PubMed Central for supplementary material.

Acknowledgments

We appreciate the assistance of A. Roque for animal husbandry.

Funding: This work was supported in part by grants KO8 AR059723 (to J.Z.) PO1 AI091580 (to J.K. and A.W.) from the National Institutes of Health, and by the Irvington Institute Postdoctoral Fellowship of the Cancer Research Institute (to Q.W.). J.D. and S.M. were supported by funding from the Research Institute at Nationwide Childrens Hospital and NIH grant AI090115 (to J.D). Author contributions: TKTKTK.

References and Notes

1. Kurosaki T, Shinohara H, Baba Y. B cell signaling and fate decision. Annu Rev Immunol. 2010; 28:21–55. [PubMed: 19827951]
2. Hermiston ML, Zikherman J, Zhu JW. CD45, CD148, and Lyp/Pep: critical phosphatases regulating Src family kinase signaling networks in immune cells. Immunol Rev. 2009; 228:288–311. [PubMed: 19290935]
3. Shiue L, Zoller MJ, Brugge JS. Syk is activated by phosphotyrosine-containing peptides representing the tyrosine-based activation motifs of the high affinity receptor for IgE. J. Biol. Chem. 1995; 270:10498–10502. [PubMed: 7537732]
4. Brdicka T, Kadlecek TA, Roose JP, Pastuszak AW, Weiss A. Intramolecular regulatory switch in ZAP-70: analogy with receptor tyrosine kinases. Mol Cell Biol. 2005; 25:4924–4933. [PubMed: 15923611]
5. Deindl S, Kadlecek TA, Brdicka T, Cao X, Weiss A, Kuriyan J. Structural basis for the inhibition of tyrosine kinase activity of ZAP-70. Cell. 2007; 129:735–746. [PubMed: 17512407]
6. Deindl S, Kadlecek TA, Cao X, Kuriyan J, Weiss A. Stability of an autoinhibitory interface in the structure of the tyrosine kinase ZAP-70 impacts T cell receptor response. Proc Natl Acad Sci U S A. 2009
7. Bradshaw JM. The Src, Syk, and Tec family kinases: distinct types of molecular switches. Cell Signal. 2010; 22:1175–1184. [PubMed: 20206686]
8. Geahlen RL. Syk and pTyr'd: Signaling through the B cell antigen receptor. Biochim Biophys Acta. 2009; 1793:1115–1127. [PubMed: 19306898]
9. Palacios EH, Weiss A. Function of the Src-family kinases, Lck and Fyn, in T-cell development and activation. Oncogene. 2004; 23:7990–8000. [PubMed: 15489916]
10. Kishihara K, Penninger J, Wallace VA, Kundig TM, Kawai K, Wakeham A, Timms E, Pfeffer K, Ohashi PS, Thomas ML, et al. Normal B lymphocyte development but impaired T cell maturation in CD45-exon6 protein tyrosine phosphatase-deficient mice. Cell. 1993; 74:143–156. [PubMed: 8334701]
11. Byth KF, Conroy LA, Howlett S, Smith AJ, May J, Alexander DR, Holmes N. CD45-null transgenic mice reveal a positive regulatory role for CD45 in early thymocyte development, in the selection of CD4+CD8+ thymocytes, and B cell maturation. J Exp Med. 1996; 183:1707–1718. [PubMed: 8666928]

12. Mee PJ, Turner M, Basson MA, Costello PS, Zamoyska R, Tybulewicz VL. Greatly reduced efficiency of both positive and negative selection of thymocytes in CD45 tyrosine phosphatase-deficient mice. Eur J Immunol. 1999; 29:2923–2933. [PubMed: 10508267]
13. Stone JD, Conroy LA, Byth KF, Hederer RA, Howlett S, Takemoto Y, Holmes N, Alexander DR. Aberrant TCR-mediated signaling in CD45-null thymocytes involves dysfunctional regulation of Lck, Fyn, TCR-zeta, and ZAP-70. J Immunol. 1997; 158:5773–5782. [PubMed: 9190928]
14. van Oers NS, Lowin-Kropf B, Finlay D, Connolly K, Weiss A. alpha beta T cell development is abolished in mice lacking both Lck and Fyn protein tyrosine kinases. Immunity. 1996; 5:429–436. [PubMed: 8934570]
15. Van Laethem F, Sarafova SD, Park JH, Tai X, Pobezinsky L, Guinter TI, Adoro S, Adams A, Sharrow SO, Feigenbaum L, Singer A. Deletion of CD4 and CD8 coreceptors permits generation of alphabetaT cells that recognize antigens independently of the MHC. Immunity. 2007; 27:735–750. [PubMed: 18023370]
16. Takata M, Sabe H, Hata A, Inazu T, Homma Y, Nukada T, Yamamura H, Kurosaki T. Tyrosine kinases Lyn and Syk regulate B cell receptor-coupled Ca2+ mobilization through distinct pathways. Embo J. 1994; 13:1341–1349. [PubMed: 8137818]
17. Turner M, Mee PJ, Costello PS, Williams O, Price AA, Duddy LP, Furlong MT, Geahlen RL, Tybulewicz VL. Perinatal lethality and blocked B-cell development in mice lacking the tyrosine kinase Syk. Nature. 1995; 378:298–302. [PubMed: 7477352]
18. Cheng AM, Rowley B, Pao W, Hayday A, Bolen JB, Pawson T. Syk tyrosine kinase required for mouse viability and B-cell development. Nature. 1995; 378:303–306. [PubMed: 7477353]
19. Cornall RJ, Cheng AM, Pawson T, Goodnow CC. Role of Syk in B-cell development and antigen-receptor signaling. Proc Natl Acad Sci U S A. 2000; 97:1713–1718. [PubMed: 10677523]
20. Saijo K, Schmedt C, Su IH, Karasuyama H, Lowell CA, Reth M, Adachi T, Patke A, Santana A, Tarakhovsky A. Essential role of Src-family protein tyrosine kinases in NF-kappaB activation during B cell development. Nat Immunol. 2003; 4:274–279. [PubMed: 12563261]
21. Zhu JW, Brdicka T, Katsumoto TR, Lin J, Weiss A. Structurally distinct phosphatases CD45 and CD148 both regulate B cell and macrophage immunoreceptor signaling. Immunity. 2008; 28:183–196. [PubMed: 18249142]
22. Zhu JW, Brdicka T, Katsumoto TR, Lin J, Weiss A. Structurally distinct phosphatases CD45 and CD148 both regulate B and macrophage immunoreceptor signaling. Immunity. 2008; 28:183–196. [PubMed: 18249142]
23. Chu DH, Spits H, Peyron JF, Rowley RB, Bolen JB, Weiss A. The Syk protein tyrosine kinase can function independently of CD45 or Lck in T cell antigen receptor signaling. Embo J. 1996; 15:6251–6261. [PubMed: 8947048]
24. Rolli V, Gallwitz M, Wossning T, Flemming A, Schamel WW, Zurn C, Reth M. Amplification of B cell antigen receptor signaling by a Syk/ITAM positive feedback loop. Mol Cell. 2002; 10:1057–1069. [PubMed: 12453414]
25. El-Hillal O, Kurosaki T, Yamamura H, Kinet JP, Scharenberg AM. syk kinase activation by a src kinase-initiated activation loop phosphorylation chain reaction. Proc Natl Acad Sci U S A. 1997; 94:1919–1924. [PubMed: 9050880]
26. Harwood NE, Batista FD. Early events in B cell activation. Annu Rev Immunol. 2010; 28:185–210. [PubMed: 20192804]
27. Tolar P, Hanna J, Krueger PD, Pierce SK. The constant region of the membrane immunoglobulin mediates B cell-receptor clustering and signaling in response to membrane antigens. Immunity. 2009; 30:44–55. [PubMed: 19135393]
28. Yang J, Reth M. The dissociation activation model of B cell antigen receptor triggering. FEBS Lett. 2010; 584:4872–4877. [PubMed: 20920502]
29. Treanor B, Depoil D, Gonzalez-Granja A, Barral P, Weber M, Dushek O, Bruckbauer A, Batista FD. The membrane skeleton controls diffusion dynamics and signaling through the B cell receptor. Immunity. 2010; 32:187–199. [PubMed: 20171124]
30. Liu W, Meckel T, Tolar P, Sohn HW, Pierce SK. Antigen affinity discrimination is an intrinsic function of the B cell receptor. J Exp Med. 2010; 207:1095–1111. [PubMed: 20404102]

31. Tsang E, Giannetti AM, Shaw D, Dinh M, Tse JK, Gandhi S, Ho H, Wang S, Papp E, Bradshaw JM. Molecular mechanism of the Syk activation switch. The Journal of biological chemistry. 2008; 283:32650–32659. [PubMed: 18818202]
32. Qian D, Mollenauer MN, Weiss A. Dominant-negative zeta-associated protein 70 inhibits T cell antigen receptor signaling. J. Exp. Med. 1996; 183:611–620. [PubMed: 8627172]
33. Chu DH, Morita CT, Weiss A. The Syk family of protein tyrosine kinases in T-cell activation and development. Immunol Rev. 1998; 165:167–180. [PubMed: 9850860]
34. Ottinger EA, Botfield MC, Shoelson SE. Tandem SH2 domains confer high specificity in tyrosine kinase signaling. J Biol Chem. 1998; 273:729–735. [PubMed: 9422724]
35. Batista FD, Arana E, Barral P, Carrasco YR, Depoil D, Eckl-Dorna J, Fleire S, Howe K, Vehlow A, Weber M, Treanor B. The role of integrins and coreceptors in refining thresholds for B-cell responses. Immunological reviews. 2007; 218:197–213. [PubMed: 17624954]
36. Adams CL, Macleod MK, James Milner-White E, Aitken R, Garside P, Stott DI. Complete analysis of the B-cell response to a protein antigen, from in vivo germinal centre formation to 3-D modelling of affinity maturation. Immunology. 2003; 108:274–287. [PubMed: 12603593]
37. Lavoie TB, Drohan WN, Smith-Gill SJ. Experimental analysis by site-directed mutagenesis of somatic mutation effects on affinity and fine specificity in antibodies specific for lysozyme. J Immunol. 1992; 148:503–513. [PubMed: 1729369]
38. Fleire SJ, Goldman JP, Carrasco YR, Weber M, Bray D, Batista FD. B cell ligand discrimination through a spreading and contraction response. Science. 2006; 312:738–741. [PubMed: 16675699]
39. Tsourkas PK, Liu W, Das SC, Pierce SK, Raychaudhuri S. Discrimination of membrane antigen affinity by B cells requires dominance of kinetic proofreading over serial engagement. Cell Mol Immunol. 2012; 9:62–74. [PubMed: 21909127]
40. Tsourkas PK, Somkanya CD, Yu-Yang P, Liu W, Pierce SK, Raychaudhuri S. Formation of BCR oligomers provides a mechanism for B cell affinity discrimination. J Theor Biol. 2012; 307:174–182. [PubMed: 22613800]
41. Monroe JG. ITAM-mediated tonic signalling through pre-BCR and BCR complexes. Nat Rev Immunol. 2006; 6:283–294. [PubMed: 16557260]
42. Srinivasan L, Sasaki Y, Calado DP, Zhang B, Paik JH, DePinho RA, Kutok JL, Kearney JF, Otipoby KL, Rajewsky K. PI3 kinase signals BCR-dependent mature B cell survival. Cell. 2009; 139:573–586. [PubMed: 19879843]
43. Zikherman J, Parameswaran R, Weiss A. Endogenous antigen tunes the responsiveness of naive B cells but not T cells. Nature. 2012; 489:160–164. [PubMed: 22902503]
44. Liu W, Meckel T, Tolar P, Sohn HW, Pierce SK. Antigen affinity discrimination is an intrinsic function of the B cell receptor. The Journal of experimental medicine. 2010; 207:1095–1111. [PubMed: 20404102]
45. Abel SM, Roose JP, Groves JT, Weiss A, Chakraborty AK. The membrane environment can promote or suppress bistability in cell signaling networks. J Phys Chem B. 2012; 116:3630–3640. [PubMed: 22332778]
46. Luby-Phelps K. Cytoarchitecture and physical properties of cytoplasm: volume, viscosity, diffusion, intracellular surface area. Int Rev Cytol. 2000; 192:189–221. [PubMed: 10553280]
47. Chan AC, Iwashima M, Turck CW, Weiss A. ZAP-70: A 70kD protein tyrosine kinase that associates with the TCR z chain. Cell. 1992; 71:649–662. [PubMed: 1423621]
48. Iwashima M, Irving BA, van Oers NS, Chan AC, Weiss A. Sequential interactions of the TCR with two distinct cytoplasmic tyrosine kinases. Science. 1994; 263:1136–1139. [PubMed: 7509083]
49. Johnson SA, Pleiman CM, Pao L, Schneringer J, Hippen K, Cambier JC. Phosphorylated immunoreceptor signaling motifs (ITAMs) exhibit unique abilities to bind and activate Lyn and Syk tyrosine kinases. J. Immunol. 1995; 155:4596–4603. [PubMed: 7594458]
50. Straus D, Weiss A. Genetic evidence for the involvement of the Lck tyrosine kinase in signal transduction throught the T cell antigen receptor. Cell. 1992; 70:585–593. [PubMed: 1505025]
51. van Oers NSC, Killeen N, Weiss A. Lck regulates the tyrosine phosphorylation of the T cell receptor subunits and ZAP-70 in murine thymocytes. J. Exp. Med. 1996; 183:1053–1062. [PubMed: 8642247]

52. Takata M, Sabe H, Hata A, Inazu T, Homma Y, Nukada T, Yamamura H, Kurosaki T. Tyrosine kinases Lyn and Syk regulate B cell receptor-coupled Ca^{2+} mobilization through distinct pathways. EMBO J. 1994; 13:1341–1349. [PubMed: 8137818]
53. DeFranco AL, Chan VW, Lowell CA. Positive and negative roles of the tyrosine kinase Lyn in B cell function. Semin Immunol. 1998; 10:299–307. [PubMed: 9695186]
54. Hanke JH, Gardner JP, Dow RL, Changelian PS, Brissette WH, Weringer EJ, Pollok BA, Connelly PA. Discovery of a novel, potent, and Src family-selective tyrosine kinase inhibitor. Study of Lck- and FynT-dependent T cell activation. J Biol Chem. 1996; 271:695–701. [PubMed: 8557675]
55. Yamamoto N, Takashita K, Shichijo M, Kokubo T, Sato M, Nakashima K, Ishimori M, Nagai H, Li YF, Yura T, Bacon KB. The orally available spleen tyrosine kinase inhibitor 2-[7-(3,4-dimethoxyphenyl)-imidazo[1,2-c]pyrimidin-5-ylamino]nicotnamide dihyrochloride (BAY 61-3606) blocks antigen-induced airway inflammation in rodents. J Pharmacol Exp Ther. 2003; 306:1174–1181. [PubMed: 12766258]
56. Goodnow CC, Crosbie J, Adelstein S, Lavoie TB, Smith-Gill SJ, Brink RA, Pritchard-Briscoe H, Wotherspoon JS, Loblay RH, Raphael K, et al. Altered immunoglobulin expression and functional silencing of self-reactive B lymphocytes in transgenic mice. Nature. 1988; 334:676–682. [PubMed: 3261841]
57. Kim YM, Pan JY, Korbel GA, Peperzak V, Boes M, Ploegh HL. Monovalent ligation of the B cell receptor induces receptor activation but fails to promote antigen presentation. Proc Natl Acad Sci U S A. 2006; 103:3327–3332. [PubMed: 16492756]
58. Gillespie DT. Exact Stochastic Simulation of Coupled Chemical-Reactions. Journal of Physical Chemistry. 1977; 81:2340–2361.
59. Lis M, Artyomov MN, Devadas S, Chakraborty AK. Efficient stochastic simulation of reaction-diffusion processes via direct compilation. Bioinformatics. 2009; 25:2289–2291. [PubMed: 19578038]
60. Zhang X, Gureasko J, Shen K, Cole PA, Kuriyan J. An allosteric mechanism for activation of the kinase domain of epidermal growth factor receptor. Cell. 2006; 125:1137–1149. [PubMed: 16777603]
61. Au-Yeung BB, Deindl S, Hsu LY, Palacios EH, Levin SE, Kuriyan J, Weiss A. The structure, regulation, and function of ZAP-70. Immunol Rev. 2009; 228:41–57. [PubMed: 19290920]
62. Chu DH, van Oers NS, Malissen M, Harris J, Elder M, Weiss A. Pre-T cell receptor signals are responsible for the down-regulation of Syk protein tyrosine kinase expression. J Immunol. 1999; 163:2610–2620. [PubMed: 10453000]
63. Chan AC, Irving BA, Fraser JD, Weiss A. The zeta chain is associated with a tyrosine kinase and upon T-cell antigen receptor stimulation associates with ZAP-70, a 70-kDa tyrosine phosphoprotein. Proc Natl Acad Sci U S A. 1991; 88:9166–9170. [PubMed: 1717999]
64. Liu W, Sohn HW, Tolar P, Pierce SK. It's all about change: the antigen-driven initiation of B-cell receptor signaling. Cold Spring Harbor perspectives in biology. 2010; 2:a002295. [PubMed: 20591989]
65. McKeithan TW. Kinetic proofreading in T-cell receptor signal transduction. Proceedings of the National Academy of Sciences of the United States of America. 1995; 92:5042–5046. [PubMed: 7761445]
66. Monroe JG. ITAM-mediated tonic signalling through pre-BCR and BCR complexes. Nature reviews. Immunology. 2006; 6:283–294.
67. Tsourkas PK, Baumgarth N, Simon SI, Raychaudhuri S. Mechanisms of B-cell synapse formation predicted by Monte Carlo simulation. Biophys J. 2007; 92:4196–4208. [PubMed: 17384077]
68. Altan-Bonnet G, Germain RN. Modeling T cell antigen discrimination based on feedback control of digital ERK responses. PLoS Biol. 2005; 3:e356. [PubMed: 16231973]
69. Zhang Z, Shen K, Lu W, Cole PA. The role of C-terminal tyrosine phosphorylation in the regulation of SHP-1 explored via expressed protein ligation. J Biol Chem. 2003; 278:4668–4674. [PubMed: 12468540]
70. El-Hillal O, Kurosaki T, Yamamura H, Kinet JP, Scharenberg AM. syk kinase activation by a src kinase-initiated activation loop phosphorylation chain reaction. Proceedings of the National Academy of Sciences of the United States of America. 1997; 94:1919–1924. [PubMed: 9050880]

71. Faeder JR, Hlavacek WS, Reischl I, Blinov ML, Metzger H, Redondo A, Wofsy C, Goldstein B. Investigation of early events in Fc epsilon RI-mediated signaling using a detailed mathematical model. J Immunol. 2003; 170:3769–3781. [PubMed: 12646643]

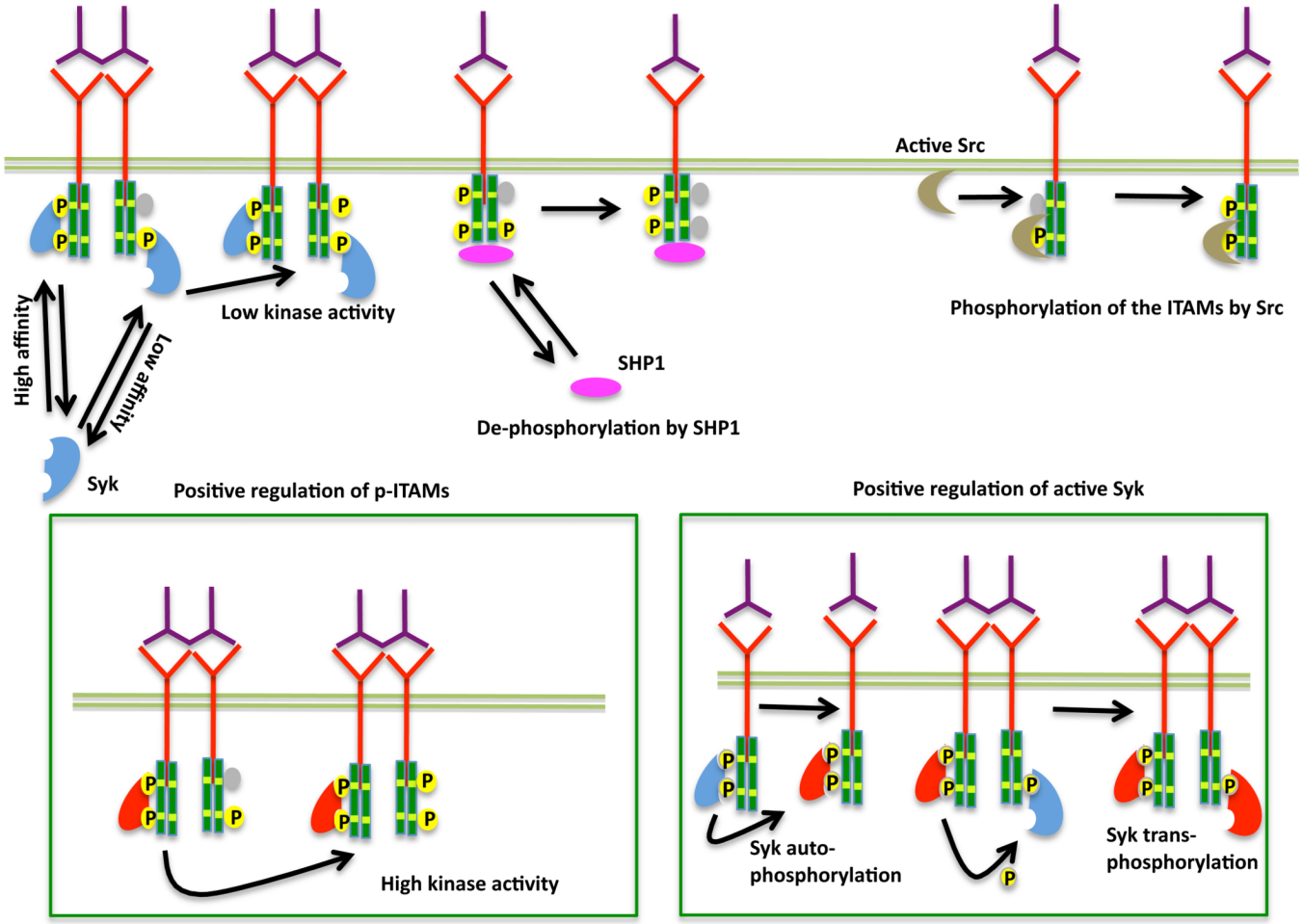

Fig. 1.

Model of membrane-proximal BCR signaling. BCRs bind to antigens and the tyrosine residues in the ITAMs associated with the antigen-bound BCRs are phosphorylated by activated forms of SFKs, such as Lyn (green crescent). Partially phosphorylated ITAMs recruit the basally active kinase Syk (in blue) with low affinity, whereas fully phosphorylated ITAMs bind to Syk with a much higher affinity. When bound to a phosphorylated tyrosine residue, Syk undergoes auto-phosphorylation at its Y348 residue and become catalytically active (in red). Catalytically active Syk, unlike ZAP-70, can also trans-phosphorylate basally active Syk that is bound to a neighboring ITAM, which constitutes a positive feedback mechanism. Moreover, when bound to an ITAM, Syk can also phosphorylate ITAMs that come in contact with its kinase domain, including those ITAMs associated with neighboring BCRs. This produces another positive feedback mechanism. The phosphatase SHP-1 (pink oval) dephosphorylates pITAMs. Binding-unbinding reactions of Src kinase domains with unphosphorylated ITAMs have been used in the model, but are not shown here for the sake of simplicity.

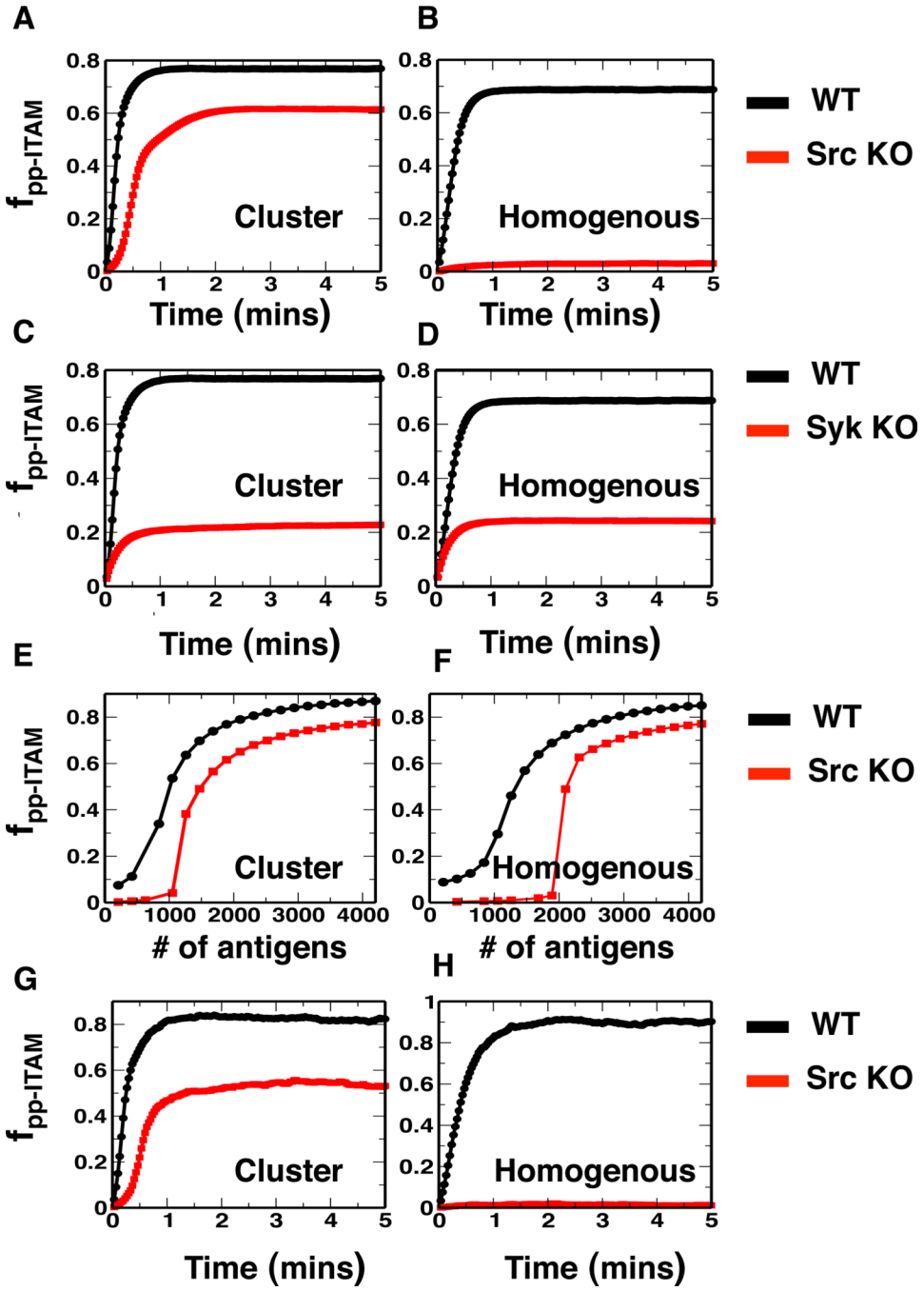

Fig. 2.

Kinetics of ITAM phosphorylation. (**A**) The kinetics of fully phosphorylated ITAMs for the wild-type (WT, black) and the SFK knockout (Src KO) (red) systems for 3 μM antigen. Under conditions of receptor clustering, the Syk feedback mechanism partially compensates for the absence of the SFKs. We used the fraction of fully phosphorylated ITAMs ($f_{pp\text{-}ITAM}$) to characterize the extent of ITAM activation. Because our model does not include serial receptor triggering, the maximum extent of ITAM activation possible in the system is twice the total number of antigens (2 × total # of antigens), and $f_{pp\text{-}ITAM}$ = the total number of fully phosphorylated ITAMs / (2 × total # of antigens). (**B**) The kinetics of fully

phosphorylated ITAMs in the WT and the SFK KO (Src KO) systems in the absence of any receptor clustering. The parameters used are the same as those in (A). (**C**) The Syk KO system (red) is compared with the WT system (black) in the presence of receptor microclusters at 3 μM antigen. In the absence of Syk, receptor clustering loses the ability to increase the extent of ITAM phosphorylation, resulting in much lower ITAM phosphorylation as occurs in the SFK KO (Src KO) system. (**D**) Kinetics of fully phosphorylated ITAMs in the WT and the Syk KO systems in the absence of any receptor clustering. The parameters used were the same as those used in (C). (**E**) The fraction of fully phosphorylated ITAMs at 4 min as the antigen concentration is increased. Receptor clustering (shown in red) in the presence of Syk produces a lower threshold of activation and partially compensates for the absence of SFKs. (**F**) Variation in the fraction of fully phosphorylated ITAMs with increasing antigen concentration in the absence of any receptor clustering. The parameters used were the same as those used in (E). (**G**) Kinetics of fully phosphorylated ITAMs for a moderate affinity antigen (k_{off}=0.05s^{-1}) in the WT and the SFK KO (Src KO) systems in the presence of receptor clustering. (**H**) Kinetics of fully phosphorylated ITAMs for a moderate affinity antigen (k_{off}=0.05s^{-1}) in the WT and the SFK KO (Src KO) systems in the absence of any receptor clustering. The parameters used were the same as those used in (G).

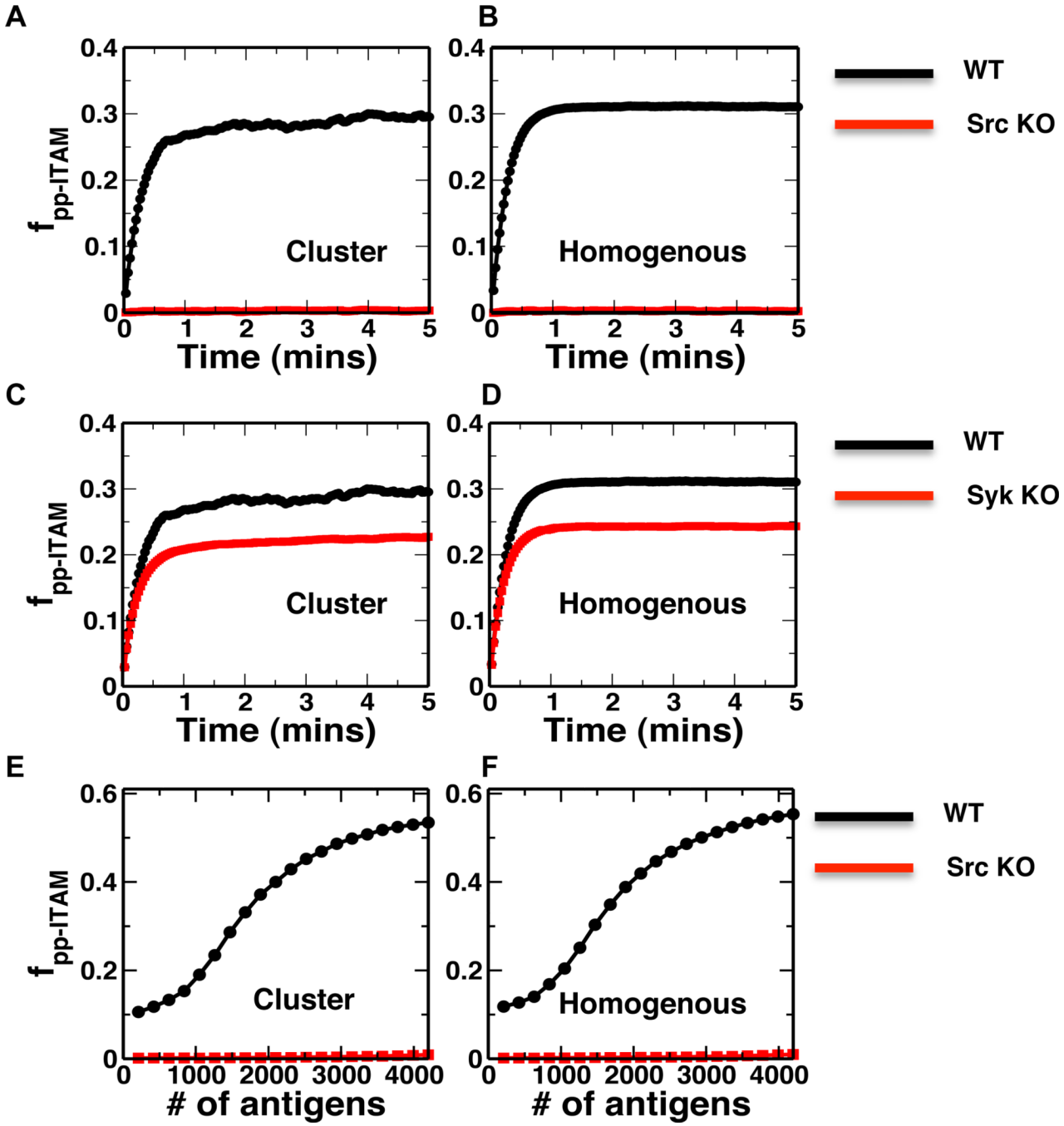

Fig. 3.

Effect of removing the Syk-mediated positive feedback from the model. (**A**) The kinetics of the fraction of fully phosphorylated ITAMs (defined in Fig. 2) in the presence of the microcluster at 3 μM antigen. The activation decreases substantially (~2-fold) in the absence of the positive feedback. For example, compare the fraction of fully phosphorylated ITAMs here with those in Fig. 2A. Receptor clustering has a negligible effect on activation in the WT or SFK knockout (Src KO) systems. (**B**) Kinetics of the fraction of fully phosphorylated ITAMs when receptor clustering is not allowed. The parameters used were the same as those used in (A). (**C** and **D**) Knockout of Syk does not affect the activation of ITAMs

substantially in the (C) presence or (D) absence of receptor clustering, because ITAM phosphorylation is mostly mediated by SFKs. (**E** and **F**) The effect of knocking out SFKs (Src KO) on the concentrations of fully phosphorylated ITAMs measured at 4 min at different antigen concentrations in (E) the presence or (F) absence of the receptor microcluster. Receptor clustering does not influence ITAM activation for the entire range of antigen concentrations.

A

	LAT		ITAM	
	Kcat (/s)	Km (uM)	Kcat (/s)	Km (uM)
Syk	1.83±0.17	212±29.1	1.21±0.04	992±67.2
Zap70	2.11±0.12	121.4±23.1	0.43±0.03	1560.5±227.3
c-Src	0.92±0.02	1086.2±79.3	3.48±0.04	416.5±41.8

B

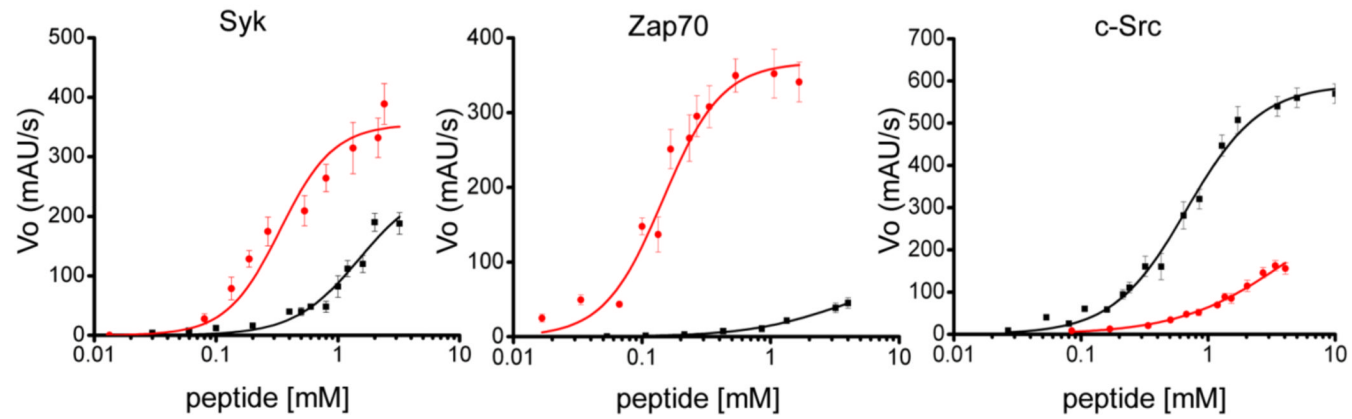

Fig. 4.

Activities and specificities of Src, Syk, and ZAP-70 for ITAM and LAT substrates. (**A**) Michaelis Menten parameters (Kcat and Km) of Src, Syk, and ZAP-70 for LAT and ITAM peptides. The two substrate peptides were derived from the region spanning Y226 in LAT (EVEEEGAPDYENLQELN) and the membrane-distal ITAM motif in the CD3ζ chain (GHDGLYQGLSTATKDTYDALHM). The values were calculated from substrate titration curves determined by an *in vitro* pyruvate-coupled assay. (**B**) Kinase specificities of Src, Syk, and ZAP-70 for ITAM (black) and LAT (red) peptide substrates. The kinase concentration was kept at 1 μM. The error bars were calculated from three independent pyruvate-coupled assay measurements.

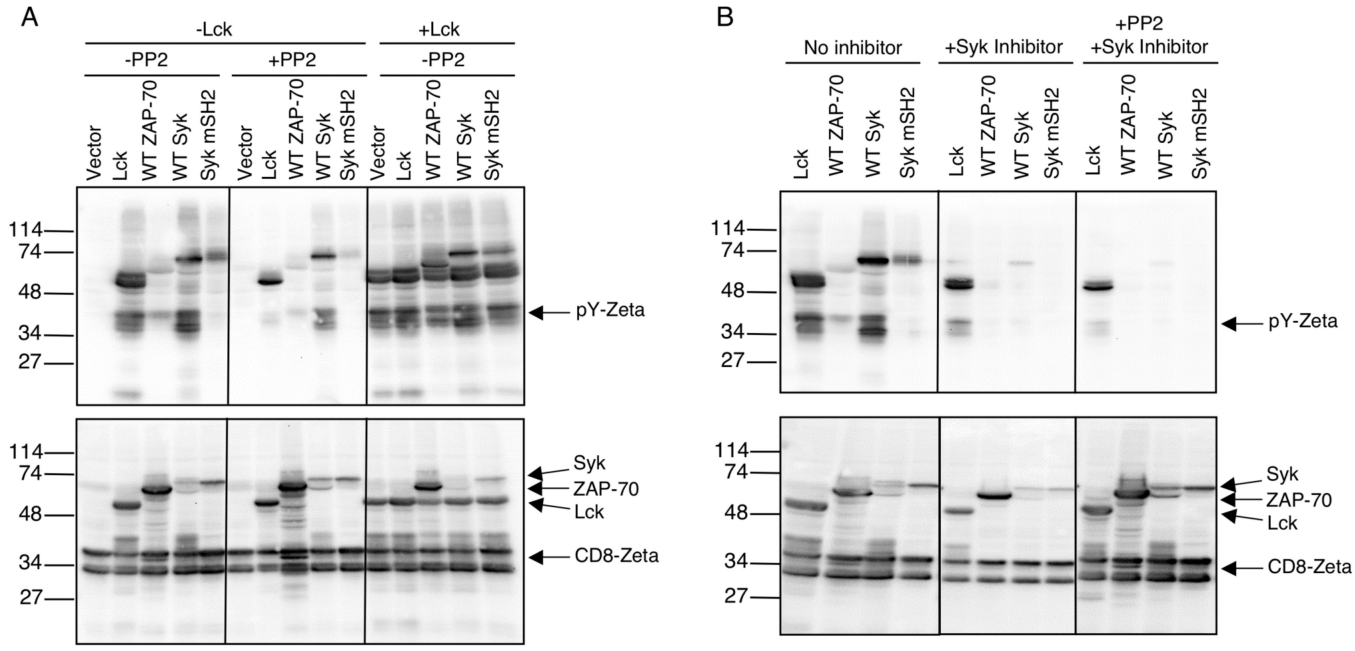

Fig. 5.

Syk, but not ZAP-70, phosphorylates ITAMs independently of SFKs. (**A** and **B**) HEK 293 cells were transiently transfected with vector control (Vector) or plasmids encoding the indicated constructs, and cells were incubated in the presence or absence of PP2 with or without Syk inhibitor for 24 hours. Whole-cell lysates were analyzed by Western blotting for total phosphorylated tyrosine content with the 4G10 monoclonal antibody (upper blots) and with a mixture of monoclonal antibodies to detect the amounts of the exogenous proteins (Lck, Syk, ZAP-70, and CD8ζ (lower blots) These data are representative of at least four independent experiments.

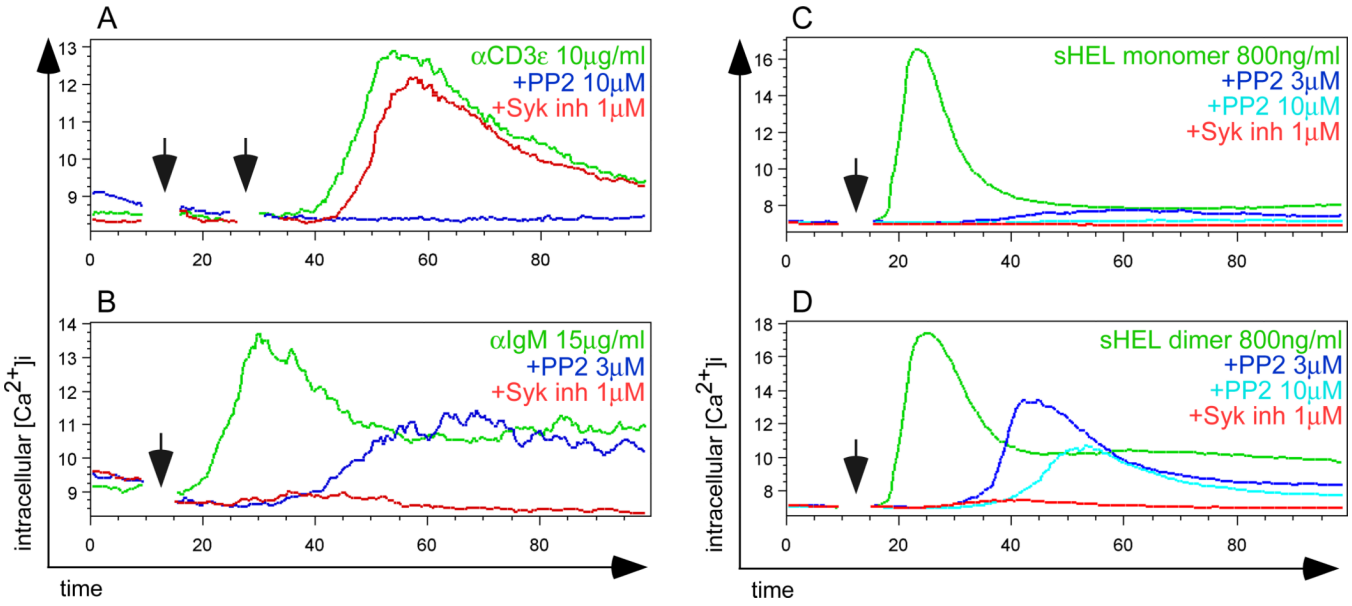

Fig. 6.

Multimeric BCR ligands permit SFK-independent BCR signaling mediated by Syk. (**A**) Indo-1-loaded primary mouse splenocytes were stimulated with anti-CD3ε antibody (first arrow) followed by cross-linking with anti-armenian hamster antibodies (second arrow) in the presence or absence of inhibitors, and changes in the intracellular free Ca^{2+} concentration were detected by flow cytometry. $CD4^+$ cells were gated to identify $CD4^+$ splenic T cells, and the ratio of Ca^{2+}-bound to -unbound Indo-1 over time was plotted. (N=5) (**B**) Indo-1-loaded primary mouse splenocytes were stimulated with anti-IgM (vertical arrow) in the presence or absence of inhibitors, and changes in the intracellular free Ca^{2+} concentration were detected by flow cytometry. $CD45R^+CD23^+CD21^{LO}$ cells were gated to identify mature splenic B cells (also known as T2 cells), and the ratio of Ca^{2+}-bound to -unbound Indo-1 over time (s) was plotted. (N=4) (**C** and **D**) Indo-1-loaded primary splenocytes from MD4 mice were stimulated with (C) sHEL monomers or (D) sHEL dimers in the presence or absence of inhibitors, and changes in the intracellular free Ca^{2+} concentration were detected by flow cytometry. $CD45R^+CD23^+CD21^{LO}$ cells were gated to identify T2 B cells, and the ratio of Ca^{2+}-bound to -unbound Indo-1 over time was plotted. Data are representative of four independent experiments.

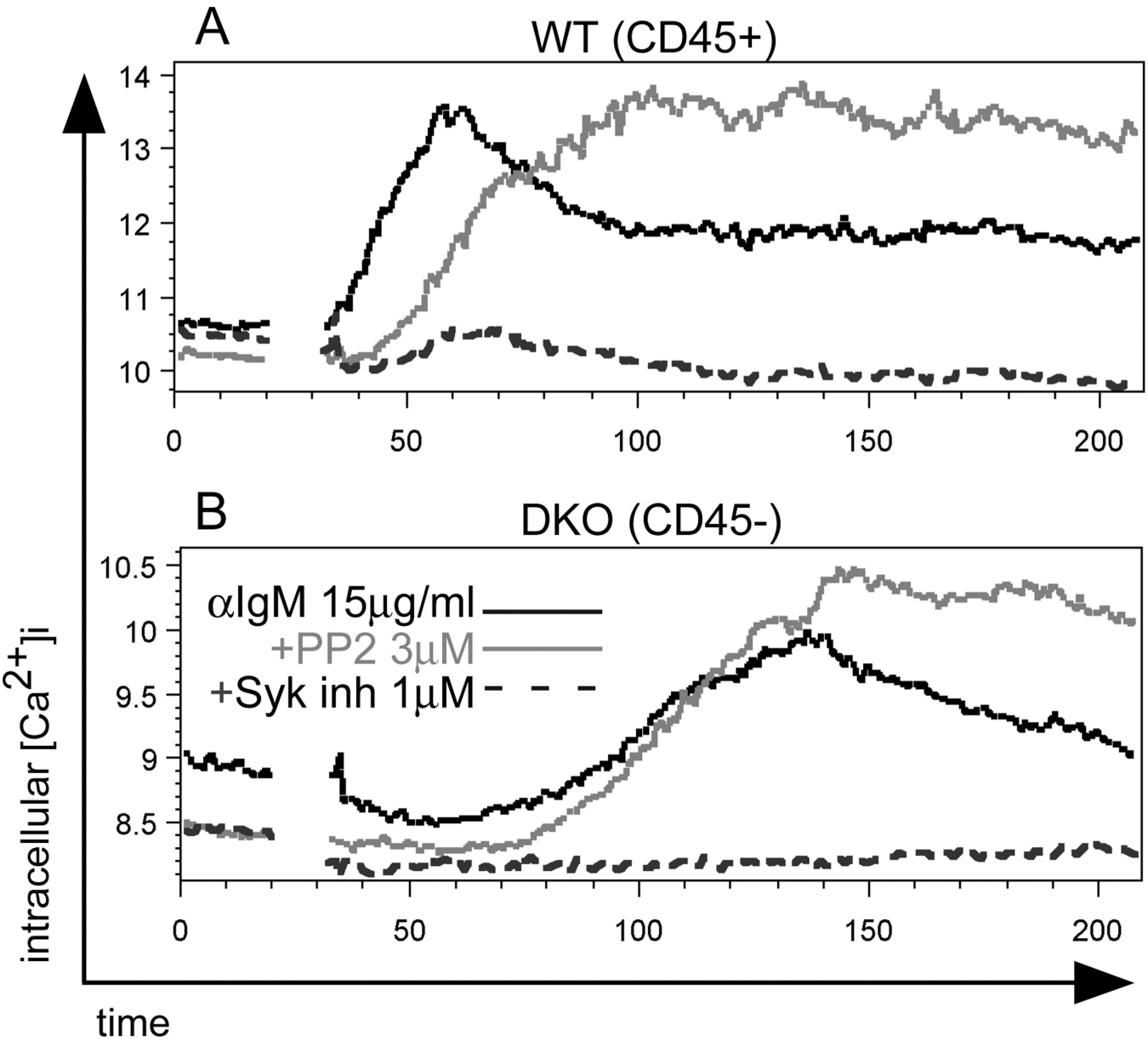

Fig. 7.

Syk mediates BCR-induced increases in intracellular free Ca^{2+} flux in CD45 and CD148 DKO B cells with genetically impaired SFK function. Lethally irradiated recipient mice were reconstituted with BM from DKO or WT control mice. Indo1-loaded B cells were stimulated with antibody against IgM in the presence or absence of inhibitors, and changes in the intracellular free Ca^{2+} concentration over time (s) were detected by flow cytometry. The responses of either WT or DKO-derived B cells were distinguished by analysis of CD45 surface expression. The ratio of Ca^{2+}-bound to -unbound Indo-1 over time was plotted. Data are representative of two independent experiments.